Original Article

Supplemental Material

Deletion of *Mocos* induces xanthinuria with obstructive nephropathy and major metabolic disorders in mice

Delphine Sedda et al.

Supplemental Methods

Histological and Immunofluorescence Analysis

Dissected tissues were fixed in 4% buffered paraformaldehyde and paraffin embedded under standard conditions. Tissue sections (3 µm) were stained with hematoxylin and eosin. The slides were examined blindly by 2 independent investigators with a Nikon microscope (Nikon eclipse 80i; Nikon, Tokyo, Japan) or with stereomicroscope (Leica M80).

For Immunofluorescence, tissues were fixed for 3 days in 4% PFA and submerged in 20% sucrose for 1 week. They were then embedded in OCT (Tissue-Teck) and 10 µM sections were prepared with cryotome (Leica). TUNEL staining was performed on sections using the ApopTag® Fluorescein In Situ Apoptosis Detection kit (Merck, S7110) following manufacturer's protocol. For Ki67 (PCNA) staining, slides were incubated 30 min in citrate buffer at 80 °C, washed in TBS-Tween and then incubated overnight with rabbit-anti-mouse-Ki67 (Abcam, 4 µg/ml, ab15580). After washing with slides were treated with 0,05% pontamin sky blue (Sigma) for 15 min and then incubated with secondary goat anti-rabbit antibody (Abcam ,2µg/mL, ab150077) for 45 min at room temperature. After washing, slides were

incubated with DAPI (Fisher Scientific) and mounted in fluoromount® (SouthernBiotech). Tissue sections were analysed on a Leicafluorescence microscope Leica (Leica, CTR6000) at x200 magnification. The slides were analyzed and semi-quantitatively scored.

Metabolic analysis

Metabolic analysEs were performed by liquid chromatography coupled with high resolution mass spectrometry (LC-HRMS) based on standard metabolomics approaches. Briefly, frozen kidney tissue samples were lyophilized during 48 h and milled to a fine powder. Two milligrams of ground samples were extracted with 1.5 mL of Methanol/milliQ water (1/1). After centrifugation, the supernatants were collected and concentrated at 35°C for 2h30. the analyses were done on a UPLC Ultimate 3000 system (Dionex), coupled to a Q-Exactive mass spectrometer (Thermo Fisher Scientific, Germany) and operated in positive (ESI+) and negative (ESI−)electro spray ionization modes. Chromatography was carried out with a PhenomenexKinetex1.7mXB C18 (150mm×2.10mm) and 100Å UHPLC column. The solvent system comprised mobile phase A [0.1% (vol/vol) formic acid in water], and mobile phase. Data were processed using Xcalibur® software (Thermo Fisher Scientific, San Jose, CA). A library of standard compounds (Mass Spectroscopy Metabolite Library of Standards MSMLS supplied by IROA TechnologiesTM) were analyzed with the same conditions and gradient of mobile phases than those used to analyze the extracted metabolites. For data processing, briefly, peaks with greater than 30% variance (CV %) in quality control samples were removed. The normalization was done to the total area of the peaks of interest. The multivariate analyses were done using Simca-P+-15 software (Umetrics, Umeå, Sweden) as previously described[36]. Briefly, the data analyses were first conducted using principal component analysis (PCA) to detect outliers. Discriminant metabolites were obtained after orthogonal partial least squares discriminant analysis (OPLS-DA), after elimination of metabolites with low impact in the

separation of the different groups. The listing of discriminant metabolites [very important in projection (VIP)] is given in supplementary data, Table S1. Univariate analyses were performed as non-parametric tests (Wilcoxon rank-sum test) using the web free server Metaboanalyst (https://www.metaboanalyst.ca/) with an FDR adjusted p-value of 0.05 (see listing of significant metabolites in supplementary data, Table S1). VIP and significant metabolites were introduced in pathways analysis module in MetaboAnalyst. Pathways showing the lowest p-value, with an impact value different from zero were chosen from the pathway topology analysis.

Legends of Supplemental figures

Supplemental Figure 1.

Heterozygous Mocos mice develop normally but *Mocos* KO mice display major morphologic abnormalities in kidney, liver and brain. (**A**) Body weight evolution in adult heterozygous *Mocos* mice and wild type littermates of 8, 10 and 12 month of age. (**B**) Pictures showing the small size and irregular surface of a *Mocos*$^{-/-}$ kidney (by planimetry the size of *Mocos*$^{-/-}$ kidneys are reduced by 50 % on average when compared to controls). (**C**) *Mocos* KO mice (n=10) had significantly decreased kidney weights and kidney to body weight ratios, compared with their control littermates at 4 weeks of age (n=6). (**D-H**) Organ weight and organ//body weight ratio were all assessed in mice at 4 weeks of age. Data are expressed as means ± SEM, **P*<0.05, ***P*<0.01, ****P*<0.001.

Supplemental Figure 2.

Deletion of *Mocos* causes occasional hydronephrosis in homozygous mutants surviving until 2 months. H&E staining of kidney sections with highly atrophic parenchymal rim (left

panel, scale bar: 1mm). The area within the rectangle is shown under higher magnification in the right panel (scale bar: 100µm).

Supplemental Figure 3.

***Mocos* disruption does not change the histology of organs except the kidney in young mice**. H&E staining of (**A**) liver and (**B**) lung sections from 4 week-old *Mocos*$^{-/-}$ mice and littermate controls (scale bar: 100µm). (**C and D**) Staining of kidney sections from 8- and 10 month-old heterozygous *Mocos* mice compared with wild type littermates. (**E and F**) Staining of liver sections from 8 and 10 month-old heterozygous *Mocos* mice compared with wild type controls (scale bar: 100µm).

Supplemental Figure 4.

Adult heterozygous *Mocos* mice display no disturbances of renal function. Analysis of serological parameters including (**A**) creatinine, (**B**) urea, (**C**) uric acid, (**D**) alanine aminotransferase (ALAT), (**E)** alkaline phosphatase and (**F**) aspartate aminotransferase (ASAT). Sera from young and adult *Mocos*$^{+/-}$ mice were compared with those from littermate control mice. Each bar represents the mean ± SEM.

Supplemental Figure 5.

Adult heterozygous *Mocos* mice exhibit normal hematological parameters. Hematological parameters of *Mocos*$^{+/-}$ mice were compared with those of wild type mice at 15- and 20- months.

Supplemental Figure 6.

Clustering result shown as heatmap for the discriminant metabolites in kidney from the 3 groups of *Mocos* $^{+/+}$, *Mocos* $^{+/-}$ and *Mocos* $^{-/-}$ mice.

Supplemental Figure 7

The purine and arginine/nitric oxide pathways in xanthinuric mice. AMP (adenosine monophosphate); IMP (inosine monophosphate); GMP (guanosine monophosphate); NO (nitric oxide); PNP1 (purine nucleoside phosphorylase1); GDA (guanine desaminase); UOX1 (urate oxidase1); OTC (ornithine transcarbamylase); NOS (nitric oxide synthase); ARG1 (arginase1); XOR (Xanthine oxidoreductase); AOX1 (aldehyde oxidase1).

Supplemental Table 1.

List of primers

Supplemental Table 2.

Listing of discriminant metabolites obtained after univariate analysis [Wilcoxon rank-sum test with an FDR adjusted p-value of 0.05, visualized by *) cumulated with VIP discriminant metabolites obtained after OPLS-DA (visualized by √), CV-ANOVA of the model was given in the first row of the table] from kidney tissues analysis of wildtype, *Mocos*$^{+/-}$ and KO mice.

Supplemental Figure 1

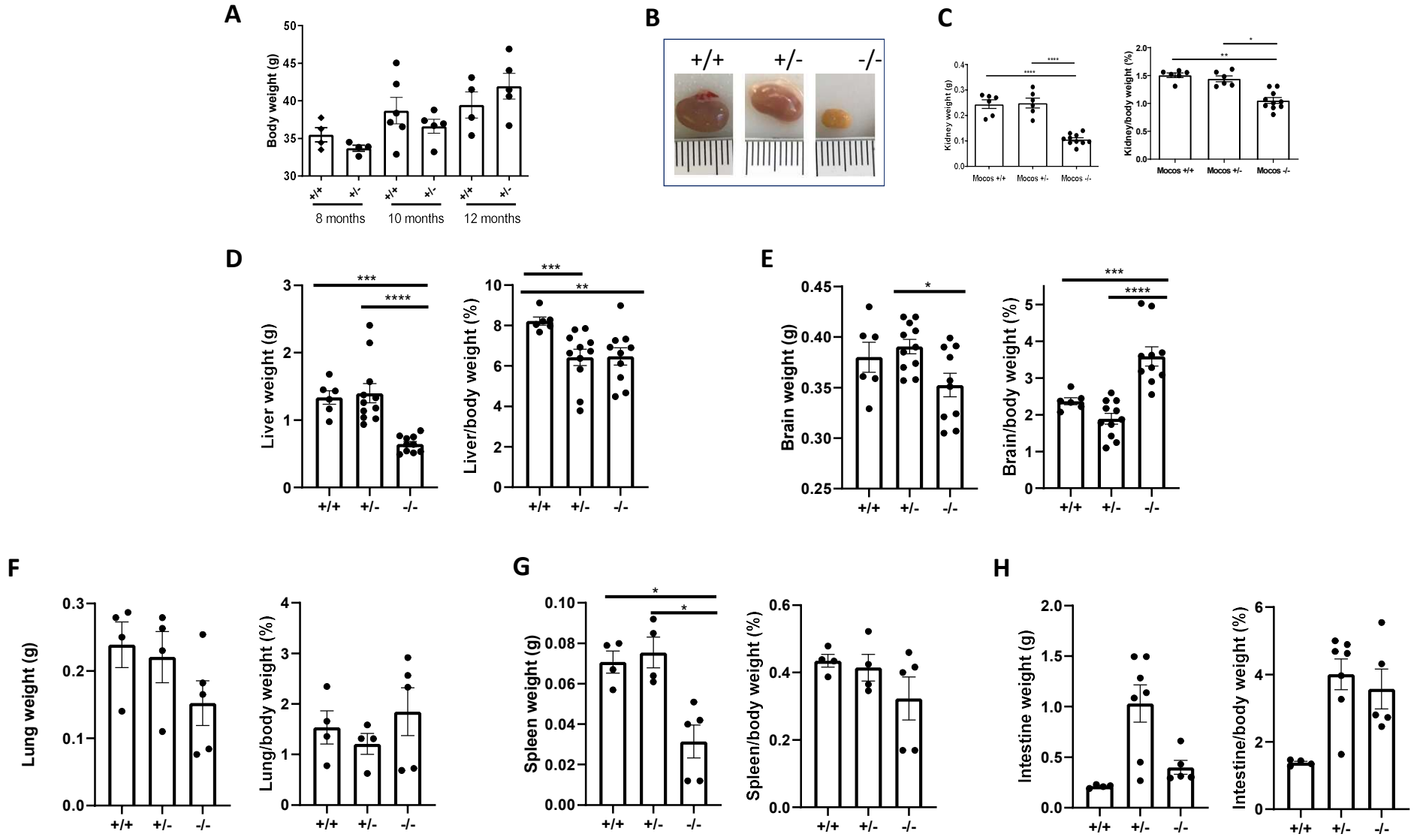

Supplemental Figure **2**

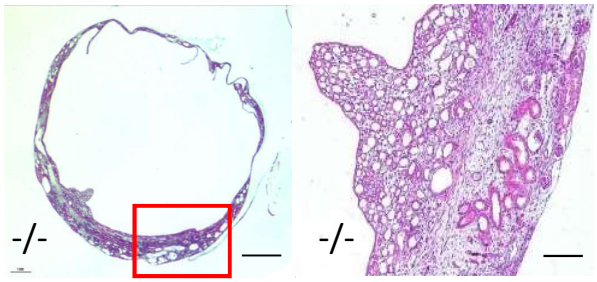

Supplemental Figure 3

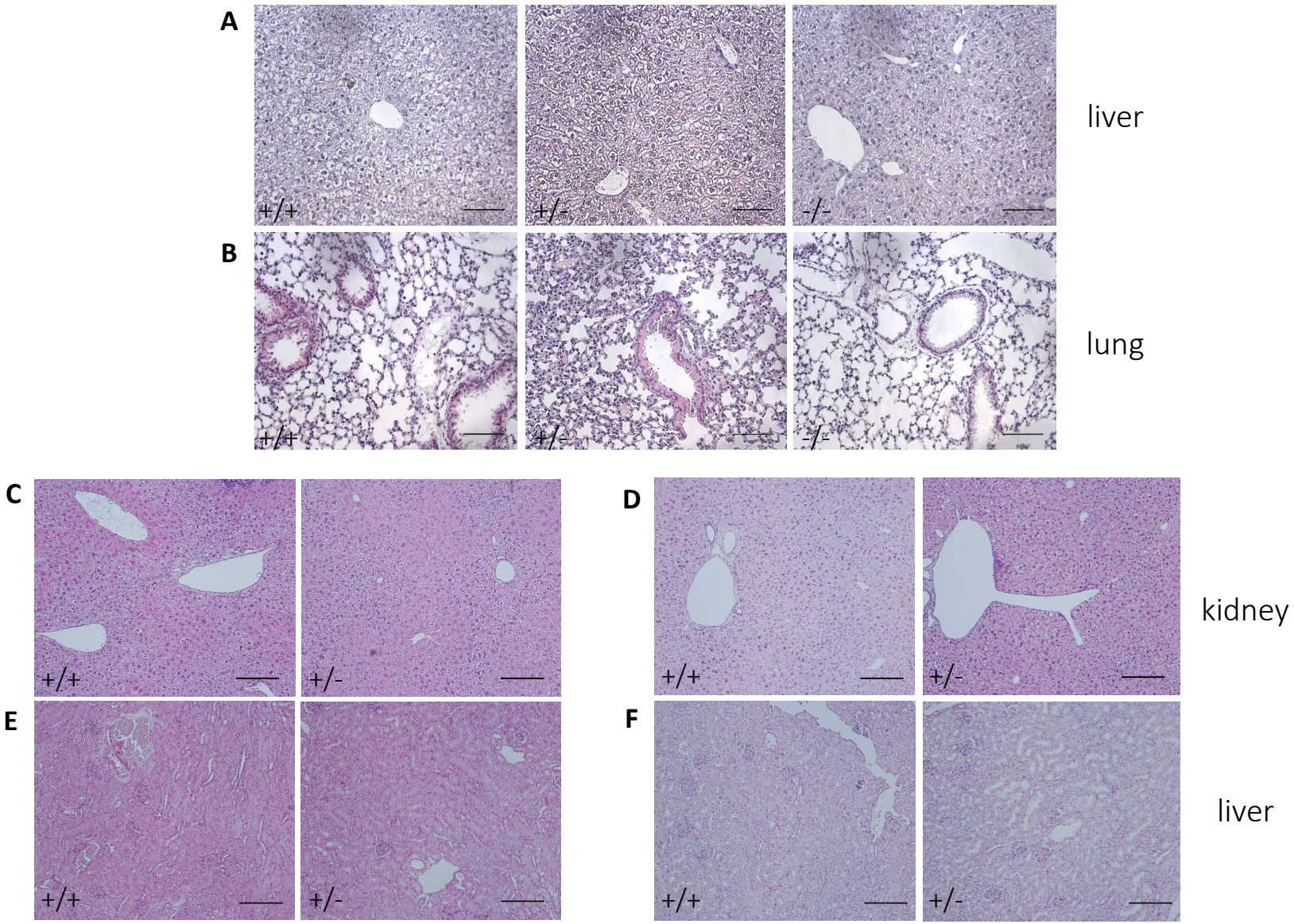

Supplemental Figure 4

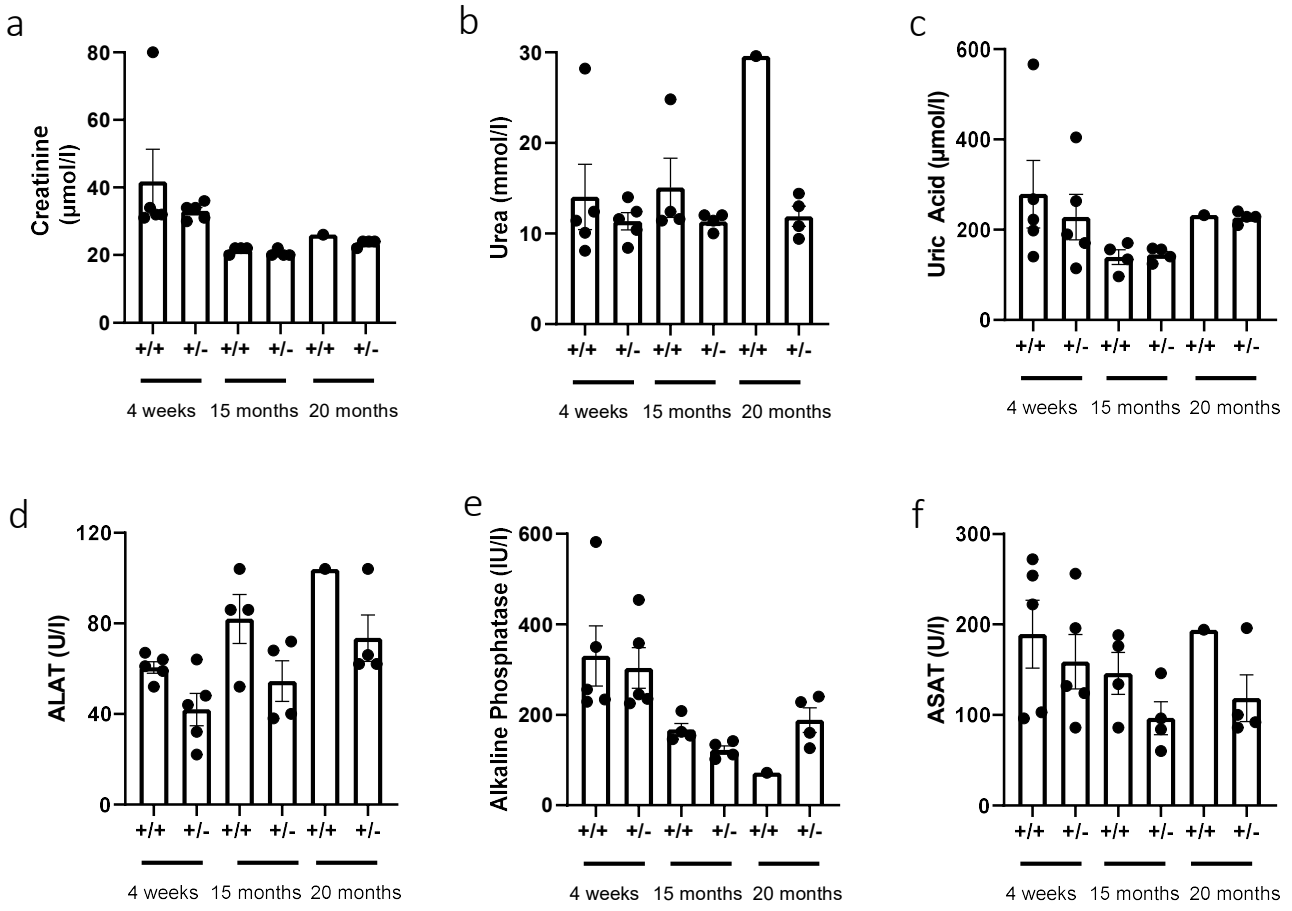

Supplemental Figure 5

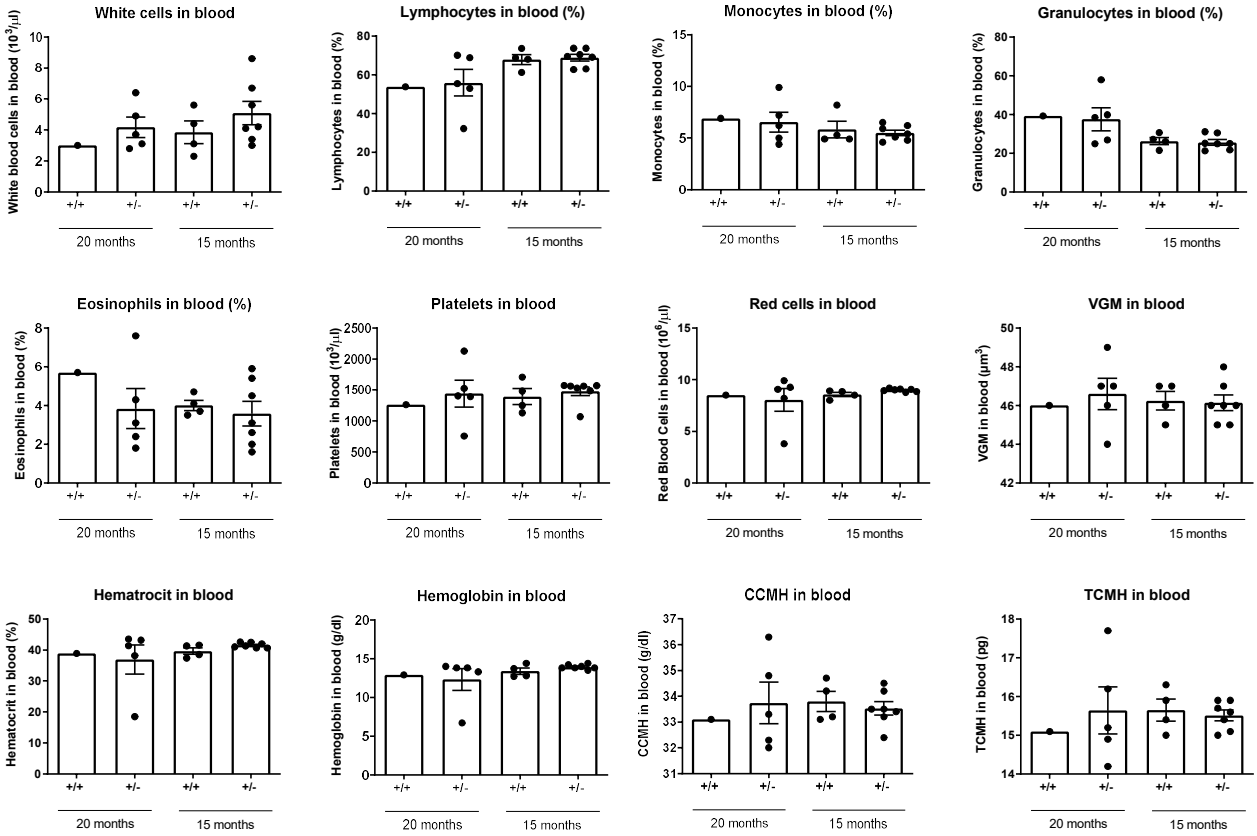

Supplemental Figure 6

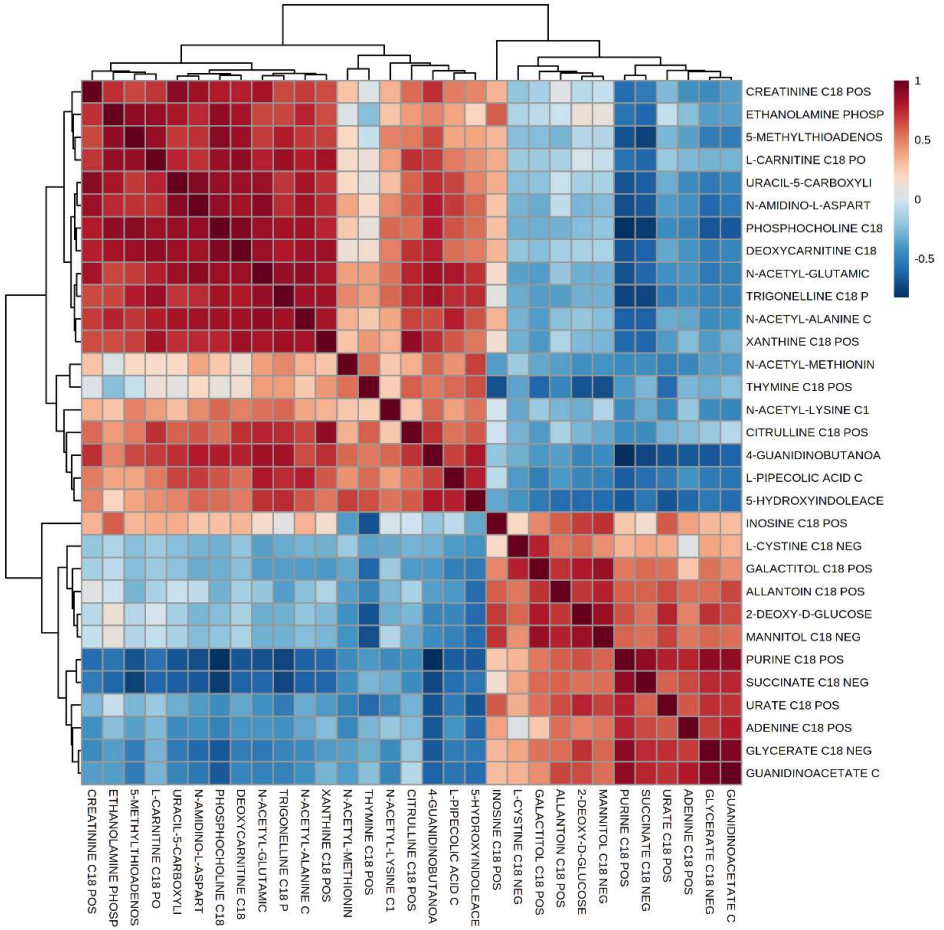

Supplemental Figure 7

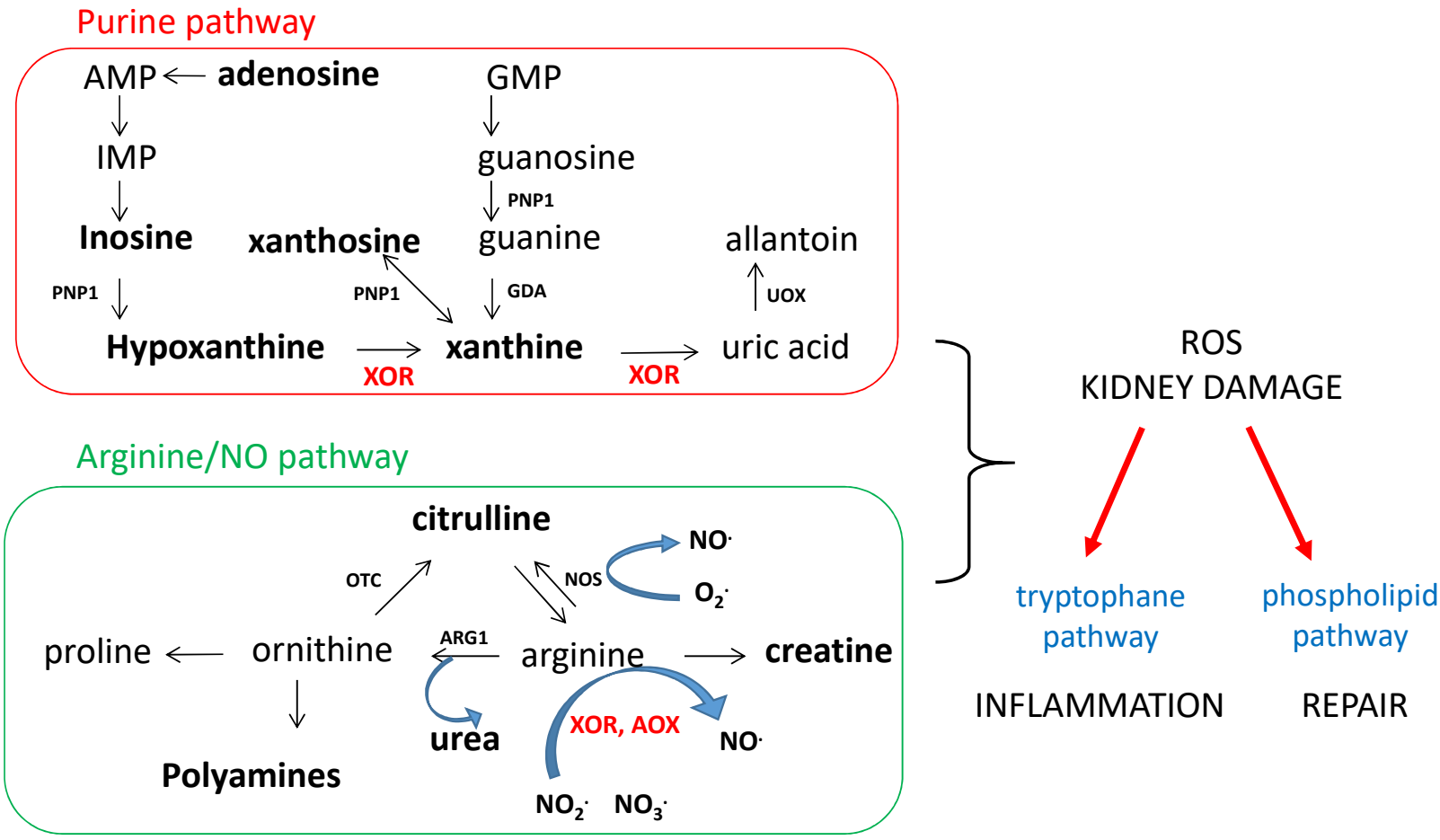

Supplemental Table 1

Mocos	*(F) 5'-CACCACCGCAGAAGACTACAC-3'* *(R) 5'-CACGTTCCGCATACCCACTAC-3'*
TNF-α	*(F) 5'-AAGCCTGTAGCCCACGTCGTA-3'* *(R) 5'-GGCACCACTAGTTGGTTGTCTTTG-3'*
MCP-1/CCL2	*(F) 5'-GCCCCACTCACCTGCTGCTACT-3'* *(R) 5'-CCTGCTGCTGGTGATCCTCTTGT-3'*
Actb	*(F) 5'-TCAGCAAGCAGGAGTACGATGAGT-3'* *(R) 5'-GGGTGTAAAACGCAGCTCAGTAACAG-3'*
Gpx1	QT01195936
Tgfβ	QT00145250
Nox4	QT00126042
Serpine1	QT00154756
Sod1	QT00165039
Tbp	QT00198443
Gclc	QT00130543
Nqo1	QT00094367
Txn1	QT01060297
Txnip	QT00296513
Txndc12	QT00141834

Akr1b8	QT00107800
Cebpb	QT00320313
Pparg	QT00100296

Supplemental Table 2

	$^{+/+}$ vs $^{+/-}$	$^{+/+}$ vs $^{-/-}$	$^{+/-}$ vs $^{-/-}$	$^{+/+}$ vs $^{+/-}$ vs $^{-/-}$
OPLS-DA CV-ANOVA	0.15	9e-012	1e-010	0.12
Metabolite				
1-OLEOYL-GLYCEROL		*		
2-DEOXY-D-GLUCOSE		*		*
4-AMINOBUTANOATE		*		
4-GUANIDINOBUTANOATE		*√	*√	
5-HYDROXYINDOLEACETATE		*√	*√	
5-HYDROXYLYSINE			*	
5-METHYLTHIOADENOSINE		*	*√	*
ADENINE		*	*	*
ALLANTOIN		*√	*√	*
ALPHA-AMINOADIPATE		*		
CITRULLINE		*	*	*
CREATININE		*	*	*
DEOXYCARNITINE		*√	*	*
ETHANOLAMINE PHOSPHATE		*	*	*
ETHYLMALONIC ACID		*		
FORMYL-L-METHIONYL PEPTIDE		*		
GALACTITOL		*	*√	*
GLYCERATE		*	*√	*
GUANIDINOACETATE		*	*√	*
INOSINE		*		*
L-CARNITINE		*	*	*
L-CYSTEIC ACID		*		
L-CYSTINE		*		*
L-PIPECOLIC ACID		*	*√	
MALATE		*		
MANNITOL		*√	*√	*
N-ACETYL-ALANINE		*	*	*
N-ACETYL-GLUTAMIC ACID		*√	*	*
N-ACETYL-LYSINE		*		*
N-ACETYL-METHIONINE		*√		*
N-AMIDINO-ASPARTATE		*	*√	*
NICOTINAMIDE MONONUCLEOTIDE		*		
PANTOTHENIC ACID		*	√	
PHOSPHOCHOLINE		*√	*√	*
PURINE		*√	*√	*
SUCCINATE		*√	*√	*
THYMINE		*		*
TRIGONELLINE		*√	*√	*

URACIL-5-CARBOXYLIC ACID		*	*√	*
URATE		*√	*√	*
XANTHINE		*		*

Listing of discriminant metabolites obtained after univariate analysis [Wilcoxon rank-sum test with an FDR adjusted p-value of 0.05, visualized by *) cumulated with VIP discriminant metabolites obtained after OPLS-DA (visualized by √), CV-ANOVA of the model was given in the first row of the table] from kidney tissues analysis of wildtype, *Mocos*$^{+/-}$ and KO mice.